IMI2 Project ID 101005077

CARE - Corona Accelerated R&D in Europe

WP6 – From lead to pre-clinical candidate and proof-of-concept in small-animal and non-human primate models

D6.7: Report on set up of the non-human primate model for SARS-CoV-2 infection and disease

Lead contributor	Participant 4_CEA
Other contributors	Participant 3_Takeda Participant 9_HZI Participant 11_KU Leuven Participant 12_LUMC Participant 14_Nuvisan

Document History

Version	Date	Description
V1	15 Feb 2021	Non-Human Primate Model for SARS-CoV-2 infection characterization and Follow-up

The CARE project has received funding from the Innovative Medicines Initiative 2 Joint Undertaking (JU) under grant agreement No 101005077. The JU receives support from the European Union's Horizon 2020 research and innovation programme and EFPIA and BILL & MELINDA GATES FOUNDATION, GLOBAL HEALTH DRUG DISCOVERY INSTITUTE, UNIVERSITY OF DUNDEE.

Table of Contents

Abstract

The objective of Task 6.4 of WP6 is to develop a non-human primate (NHP) model of SARS-CoV-2 infection and to develop the methods (viral load, immune response, inflammation, *in vivo* imaging) that will be needed for preclinical evaluation of CARE lead compounds. We have achieved the deliverable 6.7 associated to this task by demonstrating the susceptibility of macaques to a clinical isolate of SARS-CoV-2 and by the characterization of key parameters required for preclinical CARE program.

Methods

Cynomolgus macaques (*Macaca fascicularis*), aged 43-45 months and original from Mauritian AAALAC certified breeding centers were used for SARS-CoV-2 challenge studies. All animals were housed in IDMIT facilities (CEA, Fontenay-aux-roses), under BSL-3 containment (Animal facility authorization #D92-032-02, Préfecture des Hauts de Seine, France) and in compliance with European Directive 2010/63/EU, the French regulations and the Standards for Human Care and Use of Laboratory Animals, of the Office for Laboratory Animal Welfare (OLAW, assurance number #A5826-01, US). The protocols were approved by the institutional ethical committee "Comité d'Ethique en Expérimentation Animale du Commissariat à l'Energie Atomique et aux Energies Alternatives" (CEtEA #44) under statement number A20-037. The study was authorized by the "Research, Innovation and Education Ministry".

All animals were exposed to a total dose of 10^6 pfu of SARS-CoV-2 virus (hCoV-19/France/ lDF0372/2020 strain; GISAID EpiCoV platform under accession number EPI_ISL_406596) via the combination of intranasal and intra-tracheal routes (0.25 mL in each nostril and 4.5 mL in the trachea, i.e. a total of 5 mL; day 0). Nasopharyngeal tracheal and rectal swabs and blood samples were regularly collected following exposure. Broncho alveolar lavages (BAL) were performed at 3 days post exposure (d.p.e.). Blood cell counts, hemoglobin and hematocrit were determined from EDTA blood using a DXH800 analyzer (Beckman Coulter).The serum IgG directed to SARS-CoV-2 antigens were quantified using a commercially available multiplexed immunoassay developed by Mesoscale Discovery (MSD, Rockville, MD).

Viral genomic RNA (gRNA) was quantified in swabs and BAL samples by RT-qPCR with a plasmid standard concentration range. The limit of detection is estimated to be 2.67 log10 copies of SARS-CoV-2 gRNA per mL and the limit of quantification iss estimated to be 3.67 log10 copies per mL. SARS-CoV-2 E gene sub genomic mRNA (sgRNA) levels were assessed by RT-qPCR using primers with a limit of detection was estimated to be 2.87 log10 copies of SARS-CoV-2 sgRNA per mL and the limit of quantification was estimated to be 3.87 log10 copies per mL. The protocols describing the procedure for the detection of SARS-CoV-2 is available on the WHO website (https://www.who.int/docs/default-source/coronaviruse/real-time-rt-pcr-assays-for-the-detection-of-sars-cov-2-institut-pasteur-paris.pdf?sfvrsn=3662fcb6_2).

Cytokines were quantified in EDTA-treated plasma using NHP ProcartaPlex immunoassay (ThermoFisher Scientific) for IFNα, IL-1RA, IL-1β, CCL-2 (also known as MCP-1), CCL-11 (also known as eotaxin), CXCL-11 (also known as ITAC), CXCL-1 (also known as BLC), granzyme B and PDGF-BB, using NHP Milliplex (Millipore) for CD40L, G-CSF, GM-CSF, IFNγ, IL-2, IL-4, IL-5, IL-6, CXCL-8 (also known as IL-8), IL-10, IL-13, IL-15, IL-17A,

CCL-3 (also known as MIP-1α), CCL-4 (also known as MIP-1β), TNF, VEGF and a Bioplex 200 analyzer (Bio-Rad).

In vivo imaging was performed using the Digital Photon Counting (DPC) PET-CT system (Vereos-Ingenuity, Philips) (Zhang et al., 2016) implemented in BSL3 facility. CT scan was performed under breath-hold 5 minutes prior to PET scan for attenuation correction and anatomical localization. The CT detector collimation used was 64 × 0.6 mm, the tube voltage was 120 kV and intensity of about 150mAs. Automatic dose optimization tools (Dose Right, Z-DOM, 3D-DOM by Philips Healthcare) regulated the intensity. CT images were reconstructed with a slice thickness of 1.25 mm and an interval of 0.25 mm. A whole-body PET scan (4–5 bed positions, 3 min/bed position) was performed 45 min post injection of 3.39±0.28 MBq/kg of [18F]-FDG via the saphenous vein. PET images were reconstructed onto a 256 x 256 matrix (3 iterations, 17 subsets). Images were analyzed using INTELLISPACE PORTAL 8 (Philips healthcare) and 3DSlicer (Open source tool). Different regions of interest (lung, lung draining lymph nodes and spleen) were defined by CT and PET. Pulmonary lesions were defined as Ground Glass Opacity, Crazy-paving pattern or consolidation as previously described (Maisonnasse 2020). Lesion features detected by CT imaging were assessed by two analyzer independently and final CT score results were obtained by consensus. Besides, regions with FDG uptake (lung, lung draining lymph nodes and spleen) were also defined for quantification of SUV parameters, including SUVmean, SUVmax.

Results

Like the majority of patients infected with SARS-CoV2, NHPs suffered from mild clinical signs such as coughing and sneezing without dyspnoea. Clinical monitoring reveals no change in respiratory rate, oximetry and heart rate during primary infection, however temperature elevation occurs during the acute phase of infection. The viral load peaks in the upper respiratory tract between 2 to 4 days post infection (d.p.i) and is detectable in all animals at 3 d.p.i. in the lower respiratory tract (BAL). Then viral RNA decreases to undetectable level at about day 10-14 d.p.i, except in rectal fluids in which virus can remain detectable after three weeks post infection (Figure 1). Virus spike specific antibodies raised in the serum of all infected animals to reach stable values after 3-4 weeks post exposure. Six months post infection these values are in the range of the anti-S antibodies detected with the same method in plasma of convalescent patients (Figure 1). Acute infection is also characterized by increased levels of cytokines and chemokines, peaking in most of the cases between 1-3 d.p.i. This response is characteristic of early innate responses to viral infections (Figure 2).

We characterize lung inflammation and lesions with computed tomography (CT) scan (Figure 3). Typical focal ground glass opacities associated with pleural thickening with variable degrees of severity were detectable from day 2 and persisted up to day 13 in some NHPs. Infection impact in the lung lesions was further characterized by [^{18}F]-FDG uptake using PET scan combined to CT. All animals have increase glucose uptake characteristic of inflammation in the lung associated in most cases to CT observed lesions. In addition, infected animals presented an increase glucose uptake in lymph nodes draining the lung indicative of immune activation in response to SARS-CoV-2 infection (Figure 3). Iinfection was indeed followed by a transitory lymphopenia at 2 d.p.e. indicating migration of immune cells to lymph nodes and infected tissues (Figure 1).

Conclusion

The model of SARS-CoV-2 infection of cynomolgus macaques was established by the WP6 team and is now operational for testing pre-exposure prophylaxis strategies (treatment starting before infection) and post-exposure prophylaxis approaches (treatment starting between days 1 and 5 post infection). Most of the WP6 generated data within Task 6.7 is now published (Maisonnasse 2020). Infection with new viral variants, and B1.351 in particular, and lower doses are now under investigation.

Figures

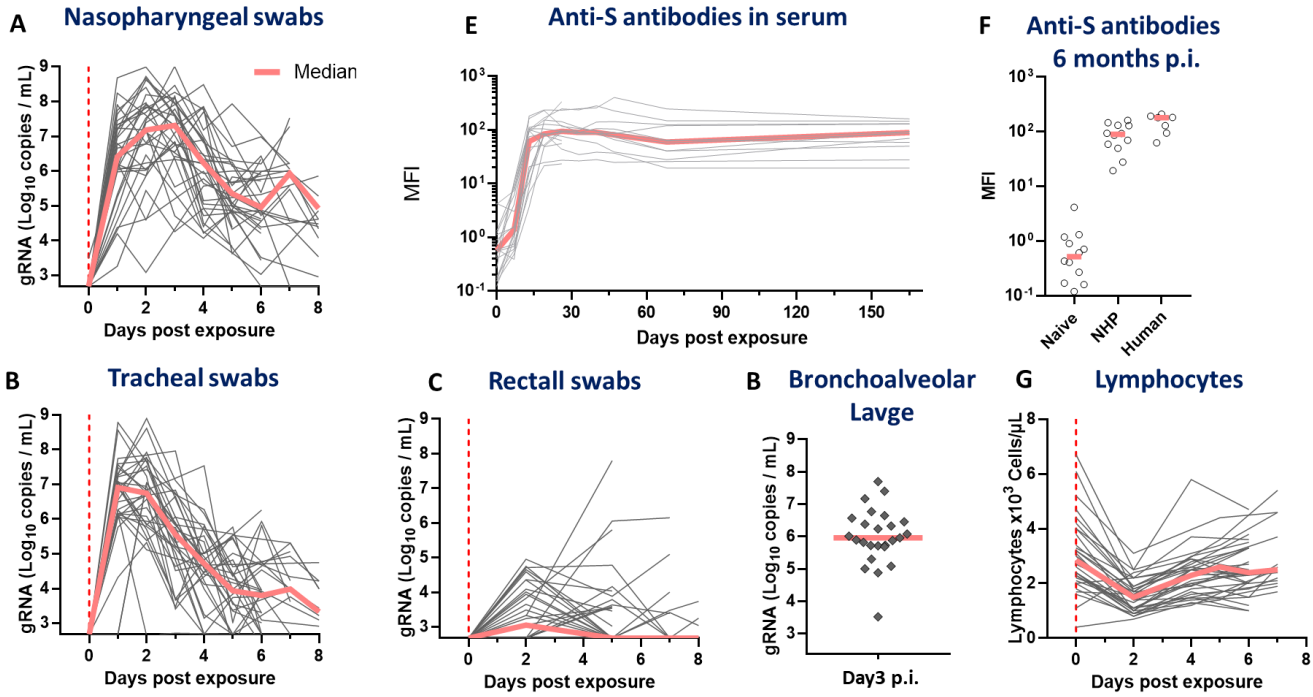

Figure 1: SARS-Cov2 challenged animals (10^6 pfu). NHPs were exposed at Day 0 (red dotted vertical line). Genomic viral RNA was measured in nasopharyngeal swabs (A), tracheal swabs (B), rectal swabs (C) and Broncho alveolar lavages (BAL) (D). The limit of detection was estimated to be 2.7 $\log_{10}$ copies of SARS-CoV-2 RNA per ml. Anti-S IgG measured in serum of macaques (E). Anti-S IgG measured in serum of macaques and plasma of convalescent patients at six months post infection (F). Lymphocyte counts in blood of infected macaques (G). Individual data are represented in grey as well as the mean (black dotted line) and the median (orange dotted line).

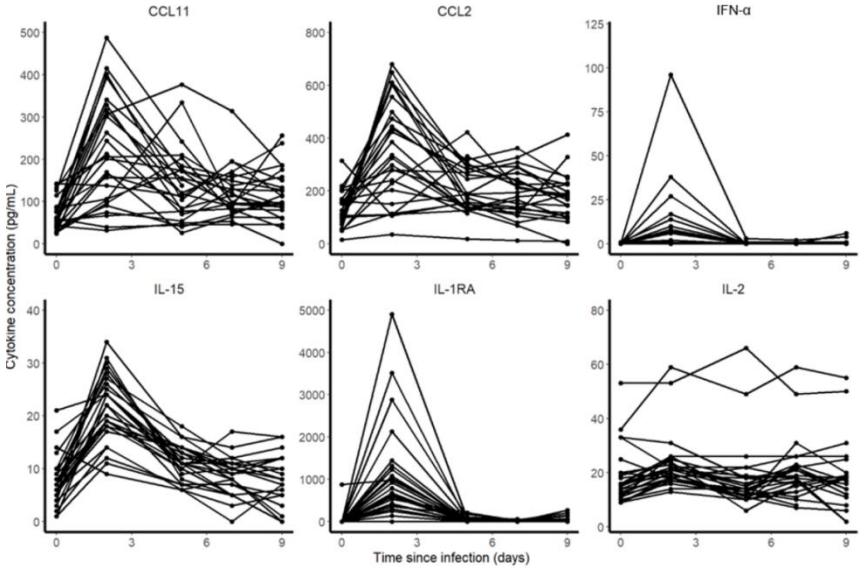

Figure 2: Illustration of cytokines and chemokines changes in plasma of macaques after SARS-Cov2 challenged animals (10^6 pfu) as measured with multiplex assays

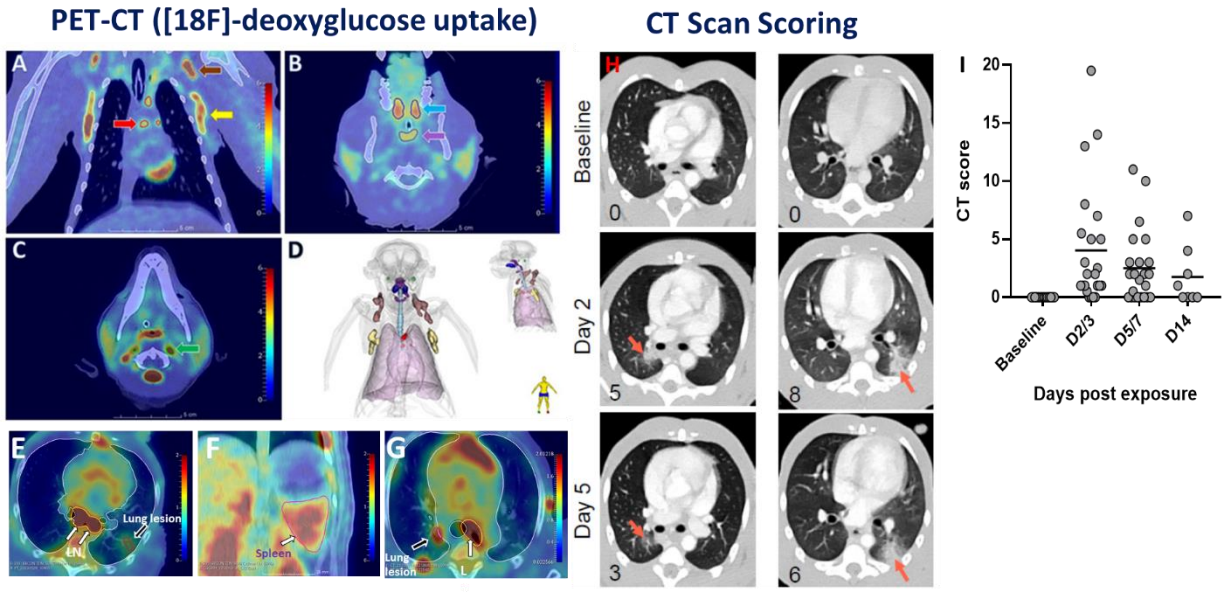

Figure 3: PET-CT images of [18F]-FDG uptake in a cynomolgus macaque. (A) Chest frontal slice with lymph node hyper metabolism in clavicular (brown arrow), mediastinal (red arrow) and axillary (yellow arrow) regions. (B-C) Transversal slice with hyper metabolism in tonsil (blue arrow), naso-pharynx associated lymphoid tissue (purple arrow) and lymph node in cervical regions (green arrow). (D) 3D representation of [18F]-FDG hyper metabolism. Lung lesions were assessed by chest CT before infection with SARS-CoV-2 and at different time points post infection (H). The overall CT score includes lesion types (ground-glass opacity, crazy-paving pattern, consolidation or pleural thickening (scored from 0 to 3)) and lesion volume (scored from 0 to 4) summed for each lobe (I). Scores are consensus values from two independent evaluators.

References

Maisonnasse, P., J. Guedj, V. Contreras, S. Behillil, C. Solas, R. Marlin, T. Naninck, A. Pizzorno, J. Lemaitre, A. Gonçalves, N. Kahlaoui, O. Terrier, R. H. T. Fang, V. Enouf, N. Dereuddre-Bosquet, A. Brisebarre, F. Touret, C. Chapon, B. Hoen, B. Lina, M. R. Calatrava, S. van der Werf, X. de Lamballerie and R. Le Grand. "Hydroxychloroquine use against SARS-CoV-2 infection in non-human primates." *Nature.* 2020. 585(7826): 584-587.